A continuum framework for grain boundary diffusion in thin film/substrate systems

Ayas, Can; van der Giessen, Erik

Published in:
Journal of Applied Physics

DOI:
10.1063/1.3488897

Publication date:
2010

A continuum framework for grain boundary diffusion in thin film/substrate systems

Can Ayas and Erik van der Giessen[a)]
Zernike Institute for Advanced Materials, University of Groningen, Nijenborgh 4, 9747 AG Groningen, The Netherlands

(Received 24 February 2010; accepted 12 August 2010; published online 6 October 2010)

A two-dimensional continuum model is developed for stress relaxation in thin films through grain boundary (GB) diffusion. When a thin film with columnar grains is subjected to thermal stress, stress gradients along the GBs are relaxed by diffusion of material from the film surface into the GBs. The transported material constitutes a wedge and becomes the source of stress inside the adjacent elastic grains that are perfectly bonded to the substrate. In the model, the coupling between diffusion and elasticity is obtained by numerically solving the governing equations in a staggered manner. A finite difference scheme is used to solve the diffusion equations, modified in order to implement realistic boundary conditions, while the elasticity problem is solved with the finite element method. The solutions reveal the existence of a universal power law scaling between the unrelaxed fraction of stress and the grain aspect ratio. For slender grains, the GB wedge attains a more uniform shape and relaxation is more effective. The kinetics of the process depends not only on the grain aspect ratio but also strongly on the thickness of the film. In case there is no adhesion between film and substrate, complete stress relaxation is attained albeit at a slightly slower rate.
 [doi:10.1063/1.3488897]

I. INTRODUCTION

Metallic thin films with thickness on the order of micrometers or smaller are routinely used in microelectronic device technology. While their main role is electric transport, mechanical properties are important for the reliability of the device.

One of the most common types of loads in thin films is due to the thermal expansion mismatch between film and substrate upon temperature change. When the thermal stress exceeds a certain threshold level, it is relaxed by inelastic processes. In thin films with columnar grains, besides dislocation-mediated slip, diffusion along the GBs is a known relaxation mechanism. The scope of this study is the relaxation of thermal stresses in a film/substrate system by GB diffusion only.

Several modeling efforts have been instrumental in understanding stress relaxation of this kind. Gao *et al.*[1] presented an essentially one-dimensional continuum framework for GB diffusion. Subsequently, Guduru *et al.*[2] developed an even simpler model in which grains are regarded as parallel linear springs normal to the GBs. These models are able to capture the basics of the phenomena, but do not (or, at least, not properly) account for the microstructure of the films, i.e., the grain size and film thickness. In the present paper, a full-field two-dimensional modeling approach is proposed for nongrowing films, which we subsequently use to gain insight in the microstructural parameters that govern the degree and the kinetics of relaxation. The method involves a combination of two numerical techniques in order to efficiently deal with the peculiar boundary conditions involved. Specifically, we will show that a careful consideration of the boundary conditions becomes essential for a two-dimensional model. The boundary conditions given in Guduru *et al.*[2] are inadequate for a two-dimensional analysis and therefore cannot describe the distribution of stress across the film width.

The stress gradient between the film surface and the uppermost part of the GB produces a chemical potential gradient which is the driving force for diffusion. As diffusion progresses, the originally neighboring faces of the GB are pushed apart by the material transported from the free surface into the GB. The GB thus becomes a source of stress and strain in the system which in turn relaxes the thermal stress in the film. These elastic fields are found by solving a mechanical (linear elastic) boundary value problem (BVP). As the kinetics of the diffusion process is determined by the well-known diffusion equation together with continuity, the development of the GB displacement profile with time is a diffusional BVP. Eventually, stress gradients along the GBs vanish and diffusion halts, even though this steady state is not necessarily stress free.

In a previous article, we have presented a model for stress relaxation where GB diffusion is represented by the motion of discrete dislocations.[3] By construction, that model contains an intrinsic length scale. We will confront the findings of the two models and will demonstrate the limitations of the continuum theory due to the absence of an intrinsic length scale.

II. GOVERNING EQUATIONS

Diffusion in general is the transport of a quantity down the chemical potential gradient. For a GB with a unit normal vector $\boldsymbol{n}$, the chemical potential of an atom is given by

[a)]Electronic mail: e.van.der.giessen@rug.nl.

$$\mu = -\Omega\sigma_n, \tag{1}$$

where Ω is the volume of an atom and σ_n is the stress normal to the GB, i.e., $\sigma_n = \boldsymbol{n}\cdot\boldsymbol{\sigma}\cdot\boldsymbol{n}$. Diffusion takes place along the GB plane in accordance with Fick's law, which relates the volumetric flux denoted by $\boldsymbol{j}$ to the gradient of the chemical potential through

$$\boldsymbol{j} = \mathfrak{D}\ \text{grad}\ \sigma_n, \quad \mathfrak{D} = \frac{D\Omega\delta}{kT}. \tag{2}$$

D is the GB diffusion coefficient, δ is the thickness of the diffusion layer, k is Boltzmann's constant, and T is temperature. The effective diffusion coefficient is denoted by $\mathfrak{D}$.

Continuity along the GB requires

$$\text{div}\ \boldsymbol{j} = -\dot{\Delta}, \tag{3}$$

in which Δ is the local width of the GB wedge in the direction $\boldsymbol{n}$ and represents the material migrated from the surface (the superimposed dot denotes the time derivative). Δ also represents the displacement jump between the two originally neighboring faces of the GB. Combination of Eqs. (2) and (3) yields the governing differential equation for diffusion,

$$\dot{\Delta} = -\mathfrak{D}\ \text{div}(\text{grad}\ \sigma_n). \tag{4}$$

In the class of problems under consideration here, GB diffusion takes place concurrently with deformation of the grains. When this deformation process remains linear elastic, the governing equations consist of, respectively, the equilibrium condition, compatibility between strain ε and displacement $\boldsymbol{u}$, and the linear thermoelastic constitutive relation:

$$\text{div}\ \boldsymbol{\sigma} = 0,$$

$$\varepsilon = \frac{1}{2}(\text{grad}\ \boldsymbol{u} + [\text{grad}\ \boldsymbol{u}]^T),$$

$$\varepsilon = \mathcal{M}:\boldsymbol{\sigma} + \alpha\Delta T\boldsymbol{I}. \tag{5}$$

Here, $\mathcal{M}$ is the fourth-order elastic compliance tensor, α the thermal expansion coefficient, ΔT the temperature change, while $\boldsymbol{I}$ is the second order unit tensor.

III. PROBLEM DESCRIPTION

We consider a thin film consisting of columnar grains that is perfectly bonded to an infinitely thick substrate, as illustrated in Fig. 1. The system is in a state of plane strain perpendicular to the x_1-x_2 plane. The film has a thickness h and all grains have the same width d. An infinitely wide film is modeled by introducing a periodic computational cell in the x_1 direction which has width w; as the grains are modeled as being isotropic and the initial conditions are uniform, it suffices to consider only a single grain in the cell, i.e., $w=d$.

The system is cooled down from an initially stress-free state and, therefore, subjected to a thermal stress, which is denoted with σ_0. In practice, the thermal expansion coefficient α_f of the (metallic) film material is higher than that of the substrate material, α_s, so that the film cannot freely contract in the x_1 direction upon cooling. In the absence of any inelastic processes, this thermal stress state is uniform inside the film and is given by

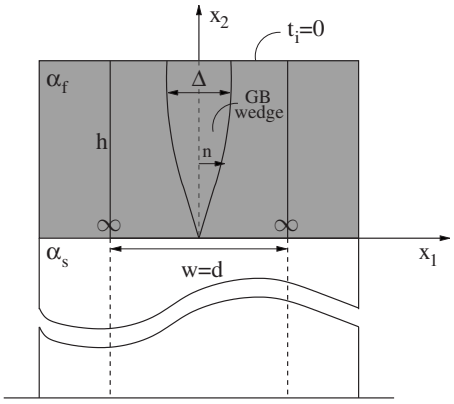

FIG. 1. Schematic illustration of the problem.

$$\sigma_{11} = \frac{(\alpha_s - \alpha_f)E\Delta T}{(1-\nu)} =: \sigma_0, \tag{6}$$

while low compressive stresses are induced in the substrate. We will investigate how this initial thermal stress relaxes by way of GB diffusion.

For this purpose we will apply the equations given in Sec. II, leading to coupled BVPs for diffusion and for elastic deformation. For their solution, numerical methods will be employed that are dedicated to the peculiar boundary conditions of the present problem. The coupling between the two BVPs is achieved by linking the numerical solution methods through the boundary conditions in a staggered manner.

A. Diffusional BVP

For the film in Fig. 1, the GB is normal to the x_1-axis, so that $\sigma_n(x_2) = \sigma_{11}(0,x_2)$ and Eq. (4) simplifies to

$$\dot{\Delta}(x_2,t) = -\mathfrak{D}\frac{\partial^2\sigma_n(x_2,t)}{\partial x_2^2}. \tag{7}$$

The boundary condition at the free surface is governed by continuity with the flux of atoms $j_{s/gb}$ migrating from the free surface into the GB,

$$j_2(h,t) = j_{s/gb}. \tag{8}$$

According to Guduru *et al.*[2] the surface flux is given by

$$j_{s/gb} = \frac{2C_s\Gamma\Omega^{5/3}}{kT}\sigma_n(h,t), \tag{9}$$

where C_s is the surface concentration of adatoms on the free surface and Γ is the jump rate of adatoms into the GB.

At the other end of the GB, material transport has to stop at the interface with the substrate, leading to the boundary condition

$$j_2(0,t) = 0, \tag{10}$$

which is equivalent to $\partial\sigma_n/\partial x_2(0,t)=0$. At the same time, however, the GB cannot open-up there since the grains are assumed to be perfectly bonded to the substrate. This gives

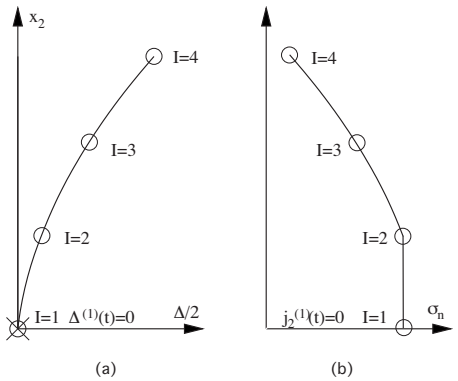

FIG. 2. Numerical implementation of (a) the perfect bonding condition Eq. (11) and (b) the zero-flux boundary condition Eq. (10) at the film/substrate interface $x_2=0$.

rise to a second boundary condition at the same point

$$\dot{\Delta}(0,t) = 0. \tag{11}$$

The conditions at the root of the GB are unusual, and therefore render this a nonstandard diffusion problem.

The diffusion Eq. (7) being constructed on the domain $[0,h]$ allows for only two spatial boundary conditions: one at the interface and one on the free surface. Having two boundary conditions at $x_2=0$, Eqs. (10) and (11), makes the BVP ill-defined from a mathematical point of view, even though they do exist physically. This difficulty was circumvented by Guduru *et al.*[2] in their one-dimensional model by prescribing only a zero stress gradient at the interface, consistent with Eq. (10). However, in a two-dimensional model, the condition $\Delta(0,t)=0$ should also be imposed to ensure compatibility in the elasticity part of the problem.

We here propose a dedicated numerical scheme to incorporate both boundary conditions Eqs. (10) and (11), which is illustrated in Fig. 2. The diffusion Eq. (7) is solved with an explicit finite difference (FD) scheme, where the GB is meshed in the thickness direction with equidistant points spaced by δx_2. The evolution of the GB wedge width Δ as a function of time in an FD scheme centered in space and forward in time is given by the following discretization:

$$\frac{\Delta^{(I)}(t+\delta t)-\Delta^{(I)}(t)}{\delta t} = -\mathfrak{D}\frac{\sigma_n^{(I+1)}(t)-2\sigma_n^{(I)}(t)+\sigma_n^{(I-1)}(t)}{\delta x_2^2}, \tag{12}$$

where δt is the time step and superscript (I) refers to grid point I. The boundary condition (11) is implemented simply by prescribing $\Delta(0,t)$ to be zero at all times in Eq. (12), see Fig. 2(a). The simultaneous implementation of the second boundary condition is achieved by modifying the FD scheme Eq. (12) at the interface. For the element at the interface a zero stress gradient is enforced by prescribing the normal stress for the second node to be equal to the normal stress for the first node at all times, i.e., $\sigma_n^{(2)}(t)=\sigma_n^{(1)}(t)$. This is illustrated in Fig. 2(b). Thus, the FD formula for the second node specializes to

$$\frac{\Delta^{(2)}(t+\delta t)-\Delta^{(2)}(t)}{\delta t} = -\mathfrak{D}\frac{\sigma_n^{(3)}(t)-\sigma_n^{(2)}(t)}{\delta x_2^2}. \tag{13}$$

To implement the flux condition (8) at the top of the GB we note that in a first-order forward difference scheme, the flux can be approximated as

$$j_2(h,t) \approx -\mathfrak{D}\frac{\sigma_n^{(N+1)}(t)-\sigma_n^{(N)}(t)}{\delta x_2}, \tag{14}$$

where N is the last grid point inside the film, i.e., $x_2^{(N)}=h$, and $N+1$ is an extra point at $x_2^{(N+1)}=h+\delta x_2$. This extra point is introduced solely to prescribe $j_2(h,t)$. Combining Eqs. (8), (9), and (14), together with identifying $\sigma_n(h,t)=\sigma_n^{(N)}(t)$, we find that the normal stress at the extra node for that time instant can be written as

$$\sigma_n^{(N+1)}(t) = \sigma_n^{(N)}(t)[1-\delta x_2/l], \quad l := \frac{\mathfrak{D}kT}{2C_s\Gamma\Omega^{5/3}}. \tag{15}$$

Here, l is a length scale that follows naturally from the analysis and which controls the surface kinetics relative to that of GB diffusion. Its value is determined by material parameters and processing conditions. The results presented subsequently are for $l=6$ nm so that $j_{s/gb}$ has the same value as considered in our previous discrete dislocation (DD) study.[3] When the diffusion coefficient is adapted from[2] as $\delta D=15\times10^2\exp(-10\,013/T)\ \mu m^3\ s^{-1}$ and the temperature is chosen to be 400 K, the value $l=6$ nm corresponds to $C_s\Gamma\approx3.31\times10^5\ s^{-1}$. For these values, surface diffusion proceeds much faster than its GB counterpart and therefore the normal stress at the uppermost part of the GB decays rapidly from σ_0 toward 0. Hence it is this boundary condition that induces the initial stress gradient between the top most part and the rest of the GB and thus initiates the diffusion process.

B. Linear elastic BVP

For plane strain conditions as considered here, the thermoelastic constitutive relation Eq. (5) becomes

$$\varepsilon_{ij} = \frac{1+\nu}{E}(\sigma_{ij}-\nu\delta_{ij}\sigma_{kk})+(1+\nu)\alpha\Delta T\delta_{ij}, \quad i,j,k\in\{1,2\}, \tag{16}$$

where E is Young's modulus, ν is Poisson's ratio, and δ_{ij} is the Kronecker delta. Periodic boundary conditions (denoted by ∞ in Fig. 1) at the sides of the cell ensure displacement and traction continuity as follows:

$$u_i(0,x_2) = u_i(w,x_2),$$
$$\sigma_{i1}(0,x_2) = \sigma_{i1}(w,x_2). \tag{17}$$

The bottom surface of the substrate is fully clamped while the film surface is traction free, i.e.,

$$u_i(x_1,0) = 0,$$
$$\sigma_{i2}(x_1,h) = 0. \tag{18}$$

The boundary conditions along the two surfaces of GB is the key to the coupling between diffusion and elasticity, as illustrated in Fig. 3(a). Due to GB diffusion, originally neighboring grain faces move apart from each other, while the gap

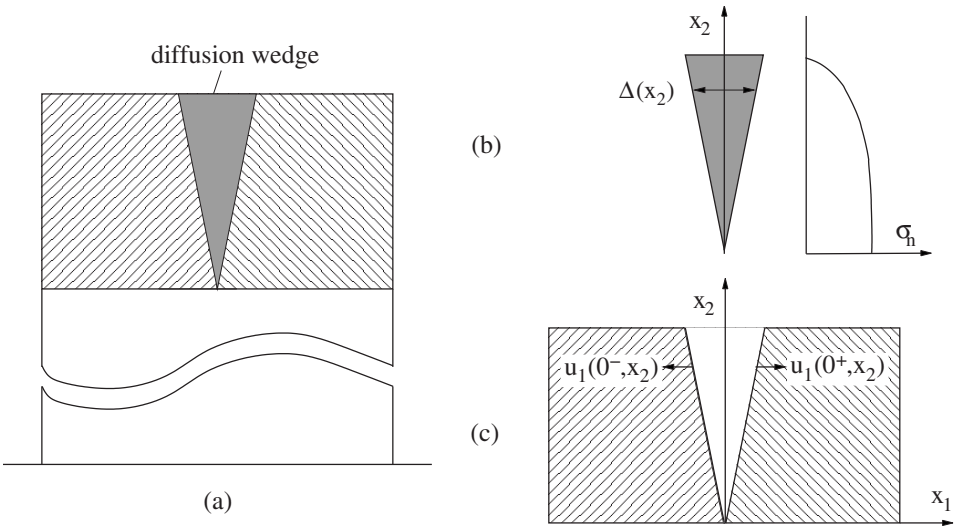

FIG. 3. The problem under consideration (a) is solved by the staggered solution of the diffusion equation under a given normal stress distribution (b) and the elasticity problem of a wedge being inserted along the GB between two elastic grains (c).

between them is filled by the GB wedge with width $\Delta(x_2)$. In our model, the GB is situated right in the center of the computational cell, hence also on the axis of symmetry (see Figs. 1 and 3). As a consequence, $\Delta(x_2)$ is equally partitioned between two neighboring grains and the shear stress along the GB vanishes by virtue of symmetry. Hence, the boundary conditions on the + and− side of the GB read

$$u_1(0^+,x_2) = \Delta(x_2)/2,$$

$$u_1(0^-,x_2) = -\Delta(x_2)/2,$$

$$\sigma_{21}(0,x_2) = 0. \tag{19}$$

Through this coupling, the solution of the diffusion problem at any time instant determines the elastic stress field inside the grains. Conversely, the corresponding GB normal stress drives the instantaneous diffusion process, cf., Eqs. (7) and (12).

The solution of the above linear elastic BVP is obtained with a standard finite element (FE) method. The FE mesh overlaps with the FD mesh on the GB and consists of quadrilateral elements that are close to being square. The film average stress $\langle\sigma_{11}\rangle^f$ is calculated by numerically integrating σ_{11} over the film elements.

C. Time integration

Since the aim of this study is to investigate the time evolution of the system, an incremental procedure is formulated in a staggered manner. The core computational task consists of two steps for every time increment, which is schematically shown in Figs. 3(b) and 3(c). In the first step, from the known stress state we solve Eqs. (7)–(11) for the diffusional BVP, and $\Delta(x_2)$ along the GB is updated for the chosen value of the time step δt. Since accommodation of the GB wedge requires displacement across the GB, the second step consists of solving the linear elastic BVP, Eqs. (16)–(19), where the field quantities u_i, ε_{ij}, and σ_{ij} are found for that particular time instant. Subsequently, time is updated and the above mentioned procedure is repeated until a steady state is established.

IV. RESULTS & DISCUSSION

Since the accuracy of the solution is intimately tied to the FD and FE mesh size, a convergence check on the element size is performed first. Figure 4 shows the relaxation of the film average stress with time for different mesh sizes. For $h=1$ μm and $d=0.25$ μm a fairly good convergence in view of the desired accuracy is attained when using 40 elements across the thickness of the film; along the x_1 direction using 20 elements renders a square FE mesh. The number of elements have been kept constant for different h values whereas the mesh size is kept constant along the x_1 direction for varying d values.

Given the chosen mesh size, the FD scheme can become unstable if δt is too large. For each film thickness, the time step is chosen to be the largest possible for a stable solution by trial and error.

The results of the simulations are reported in the subsequent three subsections. In the first subsection the focus is on

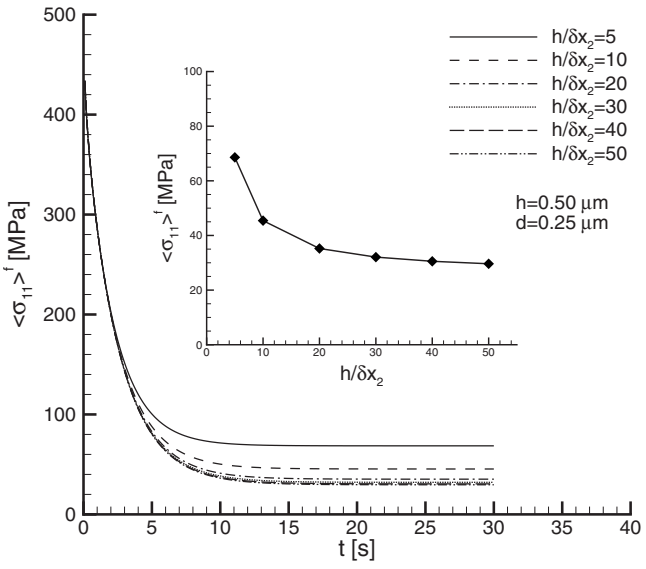

FIG. 4. Relaxation of film average stress with time in a film with grain size $d=0.25$ μm for different mesh sizes. δx_2 is the thickness of an element and h is the thickness of the film. The final, relaxed stresses for different mesh sizes are plotted in the inset.

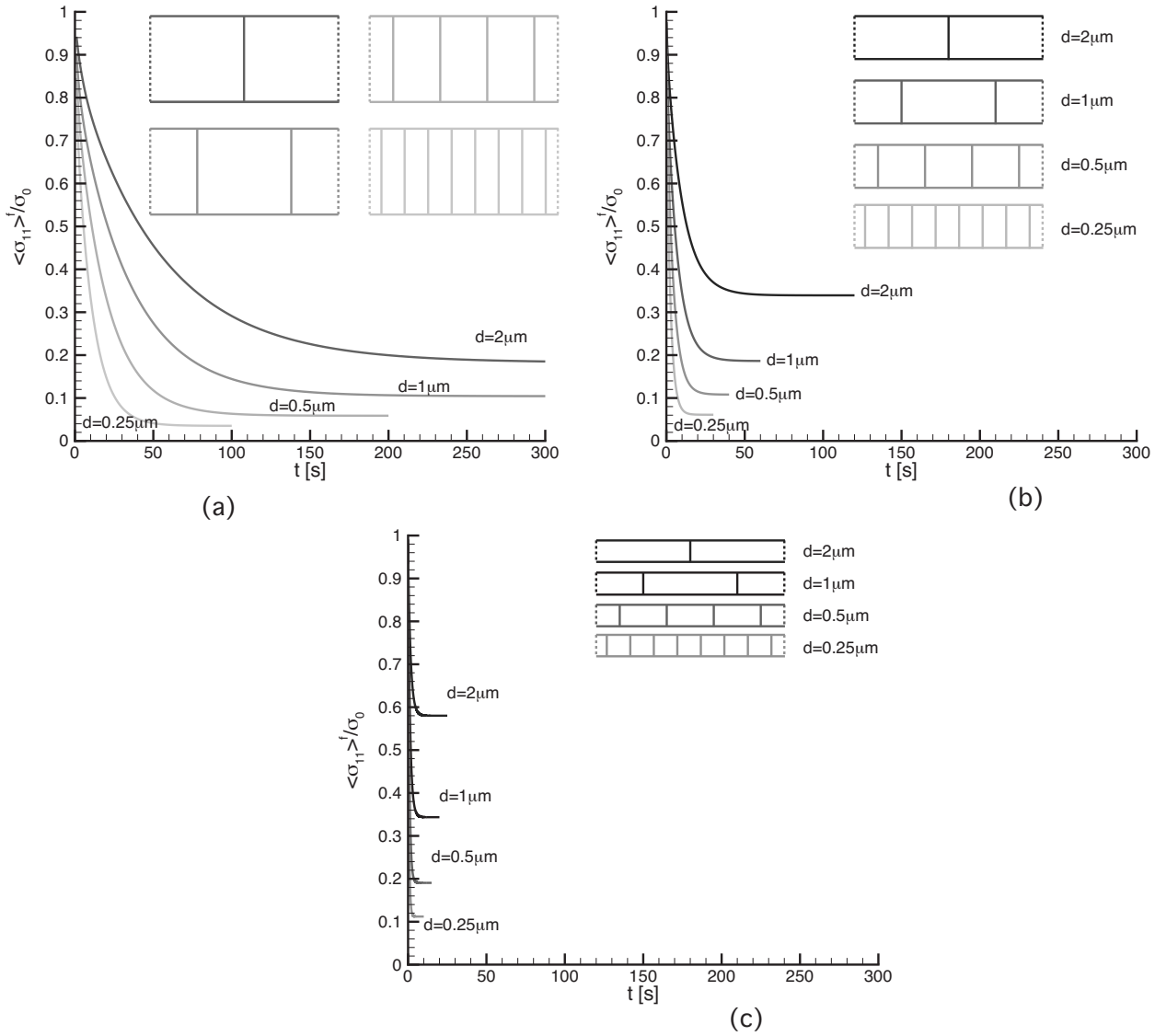

FIG. 5. Relaxation behavior from $\sigma_0=500$ MPa for different grain geometries. Thickness $h=1$ μm in (a), $h=0.5$ μm in (b), and $h=0.25$ μm in (c). Results for microstructures with the same aspect ratio h/d have the same color coding.

the identification of the parameters that control the steady state in the films, i.e., the final stress value shown in Fig. 4. Next, we investigate the kinetics of the process, which is related with the total time required for the curves in Fig. 4 to reach the steady state. Finally we will explore these features for films that are not well adhered to the substrate.

A. Steady state properties

We start by looking at the relaxation of stress in time for different grain sizes d (in the range of 0.25–2 μm) and film thicknesses h (in the range of 0.25–1 μm). The characteristic feature of all results in Fig. 5 is that all films finally reach a steady state, but at a different rate and to different stress levels.

When the Figs. 5(a)–5(c) are considered individually, the effect of grain size d for a constant film thickness h can be explored. It is clearly seen that as the grains become smaller the initial stress σ_0 is relaxed more efficiently, i.e., down to a lower residual stress level. For all the data presented in Fig. 5 the initial stress value was chosen to be $\sigma_0=500$ MPa, but this value does not have any effect on the graphs since the film average stress is normalized by σ_0. In Fig. 5, results for films with identical grain aspect ratio h/d are drawn with the same color. It is, therefore, easily recognized that films with the same aspect ratio attain the same final stress levels.

The observations above suggest there is a simple relationship between the four physical variables $\langle\sigma_{11}\rangle^f$, σ_0, h, and d. Since these four variables are expressed in terms of two basic physical dimensions (force and length), Buckingham's π theorem tells that the system is fully characterized by two linearly independent, dimensionless parameters

$$\left\{\frac{\langle\sigma_{11}\rangle^f}{\sigma_0}, \frac{h}{d}\right\}.$$

Thus, the normalized residual stress depends only on the aspect ratio of the grains.

In Fig. 6, the values of $\langle\sigma_{11}\rangle^f/\sigma_0$ for simulations with varying h and d values are compiled into a single graph. Indeed a single master curve emerges, which confirms that neither h nor d, but their ratio, controls the effectivity of

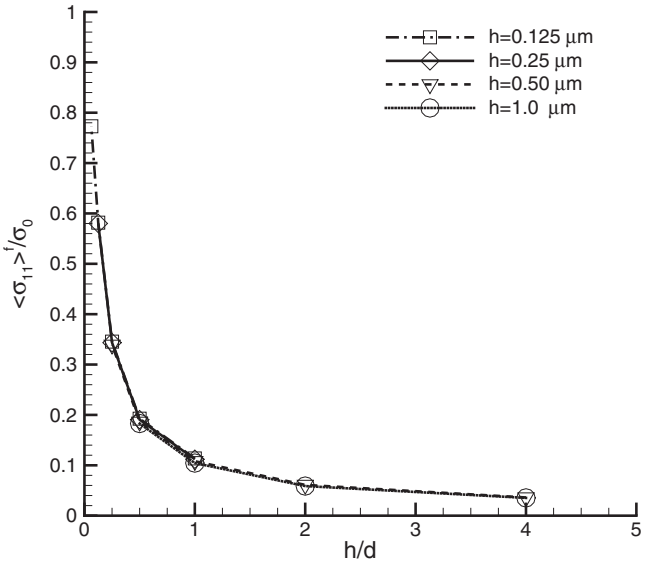

FIG. 6. Normalized residual stress values for microstructures with various h and d.

relaxation by GB diffusion. We have confirmed that the curves for different initial stress values also collapse on this master curve. Moreover, it is possible to determine the scaling law between the grain aspect ratio and the normalized residual stress by fitting the data points shown in Fig. 6 to

$$\frac{\langle \sigma_{11} \rangle^f}{\sigma_0} = c\left(\frac{h}{d}\right)^{\alpha}. \tag{20}$$

The corresponding value of the coefficient is $c=0.11$ and the exponent is found to be $\alpha=-0.77$.

Why does the effectiveness of relaxation increase with the slenderness of the grains? In our previous work[3] using DDs to model the same problem, it was found that as the grains become slender, the GB wedge attains a more rectangular shape. The same trend is observed here in the continuum solution, as seen in Fig. 7 showing the grain boundary shape parameter ξ,

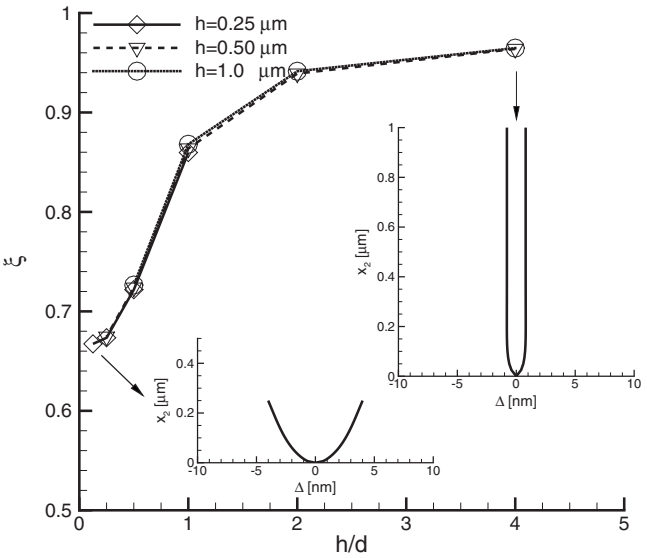

FIG. 7. Dependence of GB shape parameter ξ, according to Eq. (21), on grain aspect ratio h/d.

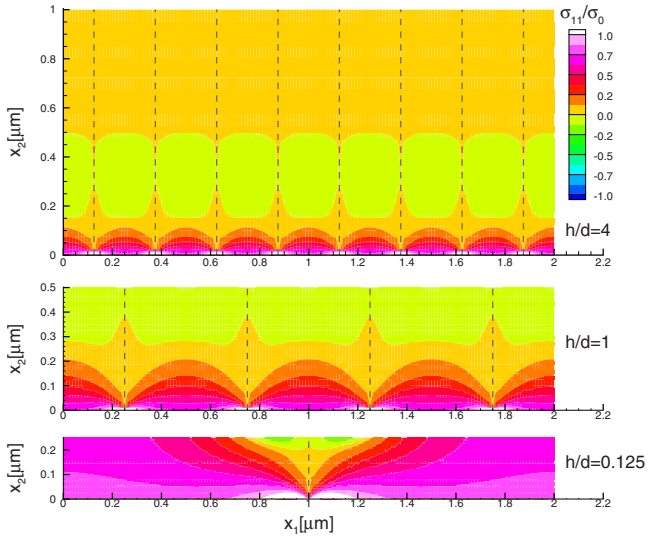

FIG. 8. (Color online) Distribution of normalized σ_{11} inside the film at steady state. The GBs are represented by light gray dashed lines.

$$\xi = \frac{1}{h\Delta(h)} \int_0^h \Delta(x_2) dx_2, \tag{21}$$

versus grain aspect ratio. The value of ξ reaches 1 for a perfect U–shaped opening, whereas for a perfect V–shaped opening $\xi=0.5$. This parameter is observed to also depend solely on the grain aspect ratio, with the value of ξ increasing from ≈ 0.7 for wide grains to 1 as the grains become more slender. Among the microstructures studied here, the film with $h=1$ μm and $d=0.25$ μm features the most uniformly shaped GB wedge (see inset of Fig. 7), while the film with $h=0.25$ μm and $d=2$ μm shows a GB opening closest to a triangular profile.

Figure 8 displays the final residual stress distributions for three different h/d. We observe large regions in between GBs where a significant amount of the initial tensile stress is still present for the widest grains ($h/d=0.125$). Effective relaxation has only taken place near the GBs. However, as the aspect ratio increases, the relatively unrelaxed area rapidly shrinks down to a thin region in the proximity of the film/substrate interface. In Fig. 9 the distribution of other stress components at steady state is shown for the case $h=d=0.5$ μm but this time only for one periodic cell. Although σ_{11} has been relaxed to a great extend as have been shown in

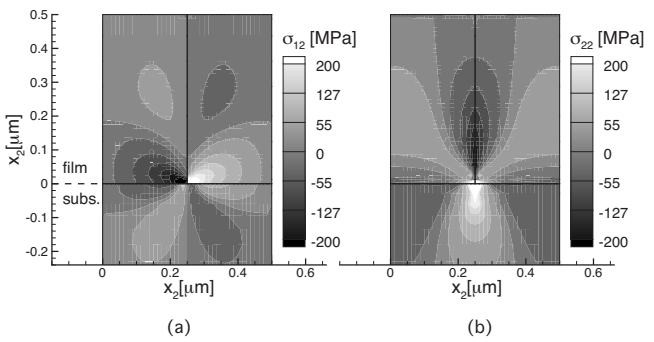

FIG. 9. Distribution of σ_{12} (a) and σ_{22} (b) within the periodic cell at steady state.

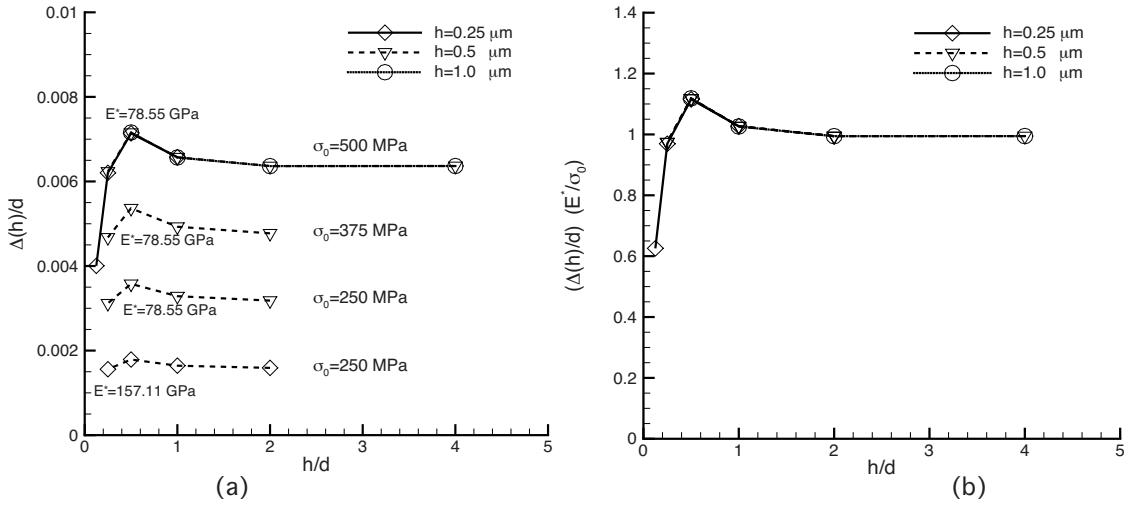

FIG. 10. GB wedge width normalized by d as a function of h/d (a). Dimensionless GB width multiplied by dimensionless elastic modulus vs h/d (b).

Fig. 8 the development of diffusion wedge builds up σ_{12} and σ_{22}. Both of these quantities are initially zero.

In addition to ξ, the effectiveness of relaxation depends on the thickness of the diffusion wedge at the top of the film. When $\Delta(h)$ is normalized with d, it gives the strain imposed as a result of diffusion at the top. The dependence of this parameter on grain aspect ratio is given in Fig. 10(a). Initially, as the aspect ratio increases the GB wedge becomes wider, but then it decreases and levels off. The h/d parameter window in which the decrease is observed coincides with the range where the ξ value increases most drastically in Fig. 7. Contrary to ξ, the GB wedge width does depend on the value of σ_0 as depicted in Fig. 10(a), as well as on the plane strain elastic modulus $E^* := E/(1-\nu^2)$. Yet Fig. 10(b) demonstrates that a master curve emerges when $\Delta(h)/d$ is multiplied with E^*/σ_0. Thus, eventually, it is these two parameters—ξ and $\Delta(h)E^*/\sigma_0/d$—that control the residual stress level as a monotonically decreasing function of aspect ratio (as in Fig. 6) in accordance with Eq. (20).

The relevance of $\Delta(h)E^*/\sigma_0/d$ in this regard can be understood by noting that if the GB wedge were perfectly U–shaped ($\xi=1$), an opening $\Delta(h)$ can be thought of as inducing an overall strain $\Delta(h)/d$ in the x_1–direction that would counteract the initial elastic strain σ_0/E^*. When $\xi \neq 1$, we have to work with the total amount of diffused material, as defined by

$$\Lambda = \int_0^h \Delta(x_2)dx_2. \tag{22}$$

This can be rewritten as $\Lambda = \xi h \Delta(h)$, leading to a diffusion-induced strain $\Lambda/(hd) = \xi\Delta(h)/d$. Based on these ideas, we postulate that the film average stress after diffusion of an amount of material Λ can be expressed as

$$\langle\sigma_{11}\rangle^f = \sigma_0 - E^*\frac{\Lambda}{hd}. \tag{23}$$

The accuracy of this relationship is confirmed in Fig. 11 which shows the correlation between the values of $\Lambda/(hd)$ and the fraction of the stress that is relaxed.

When the predictions of the continuum model above are compared with those of the DD model,[3] two notable distinctions emerge. In the continuum model relaxation will take place irrespective of the magnitude of σ_0, whereas in the DD model the initial stress should exceed a "diffusional yield strength" for the initiation of diffusion. The origin of this yield strength is the attraction of a dislocation to a nearby free surface. For a dislocation on the verge of nucleation from free surface, the attractive force may overcome the force due to tensile thermal stress and hence hinder the diffusional deformation all together.

Second, while the residual stress decreases monotonically with increasing h/d in the continuum model, it levels off after a critical h/d in the DD calculations. The critical h/d depends on the initial stress and diffusional yield strength. The origin of this barrier is the presence of a material length scale in the DD model of diffusion, namely the magnitude of the Burgers vector. This length scale constitutes the minimal admissible displacement in the GB wedge:

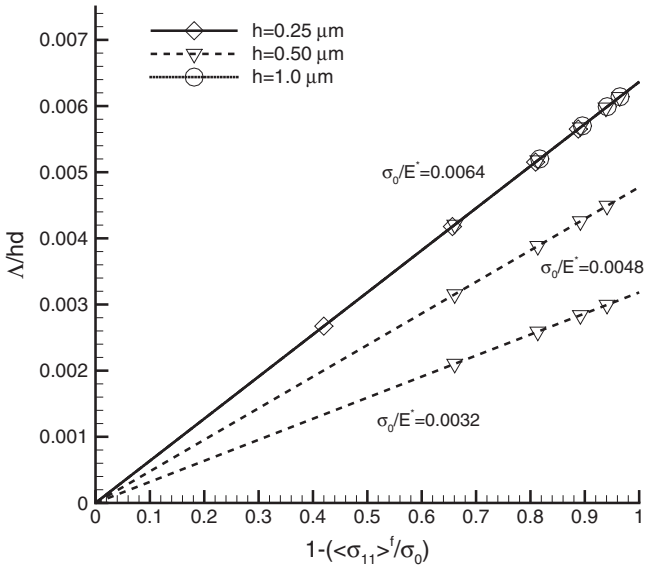

FIG. 11. Diffused material per grain area vs fraction of relaxation for different σ_0/E^* values.

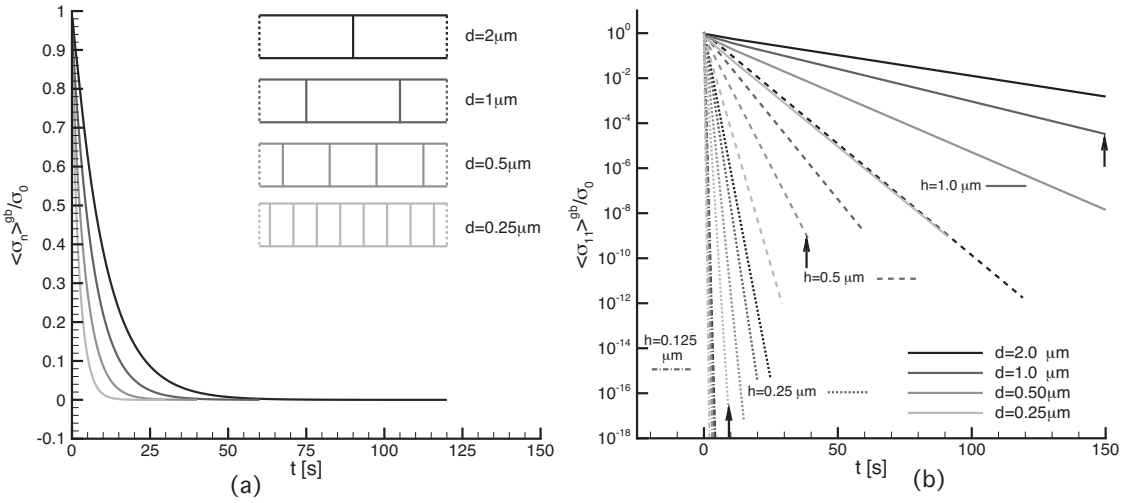

FIG. 12. Relaxation of average normal stress on the GB with time for $h=0.5$ μm (a), relaxation data for different h and d values where normalized stress is given on a logarithmic scale (b). Gray scales denote the grain size, different line types are used for different values of h.

diffusion halts when the GB cannot accommodate another extra half-plane of atoms. In the continuum model, there is no such limitation: complete stress relaxation is possible by developing a GB wedge width Δ that can be infinitesimally small. When σ_0 is high and the grains are sufficiently coarse, there is perfect agreement between the two models.

B. Kinetics

Although the amount of relaxation is the same for films comprised of grains with identical aspect ratios, the kinetics of relaxation can be very different. For instance, when the curves for $h/d=0.5$ in Figs. 5(a)–5(c) are examined, the time until completion of diffusion seems to decrease substantially as the film thickness decreases. This is expected since mass transport occurs over the length of the GBs: hence, the thinner the film, the shorter the distance the atoms have to travel, and thus the faster relaxation. Furthermore, the pace of relaxation for a constant h [see, for example, Fig. 5(a)] is seen to depend on d. As the grains become thinner, relaxation speeds up since diffusion takes place across more GBs per unit film area. However, the dependence of the diffusion rate on d seems to be weaker compared to that on h. In the remainder of this section, we want to get insight in the combined effect of h and d.

Atomistic[4] as well as continuum dislocation[1] models for GB diffusion have suggested that the GB normal stress averaged over the film thickness, $\langle\sigma_n\rangle^{\mathrm{gb}}$, decays exponentially with time,

$$\langle\sigma_n(t)\rangle^{\mathrm{gb}} = \sigma_0 \exp(-t/\tau_c), \tag{24}$$

with a characteristic time τ_c that scales as $\tau_c \propto h^{\eta}$. The value of η was found to be 3.0 with the continuum dislocation model,[1] whereas $\eta \approx 2.7$ according to the atomistic study.[4] The time decay of the average GB normal stress $\langle\sigma_n(t)\rangle^{\mathrm{gb}}$ in our computations (obtained by numerical integration of σ_{11} over the GB) is presented in Fig. 12(a). Note that, contrary to film average stress (cf. Fig. 5), the average GB normal stress does relax to zero. The difference arises from the presence of residual stresses inside the grains, as seen in Fig. 8. The relaxation curves in Fig. 12(a) fit perfectly to exponential time decay. This is confirmed by plotting the data on a logarithmic scale, see Fig. 12(b), which renders all relaxation curves as straight lines passing through the origin and having a slope

$$\ln(\langle\sigma_n\rangle^{\mathrm{gb}}/\sigma_0)/t = -1/\tau_c. \tag{25}$$

Our aim now is to find the relation between τ_c and film thickness h according to the present model. For this, we first note that dimensional considerations of the governing parameters—$\mathfrak{D}$ in (7), E in (16) and the various variables with dimension length—dictate that only the ratio of length to the power 3 divided by $E\mathfrak{D}$ has the proper dimension of time. Hence, τ_c scales with a length scale to the power 3. A model with only h as a length scale necessarily leads to $\eta \propto h^3$ as given in,[1] but the present model also involves the grain width d and the material length scale l, defined in Eq. (15). Observing that the grain width has entered the results so far only through the grain aspect ratio h/d, we postulate the following functional dependence:

$$\tau_c = h^{\eta} l^{(3-\eta)} f(h/d)/(E\mathfrak{D}), \tag{26}$$

with f a function to be established. By considering relaxation curves for the same aspect ratio but different thickness, (for example, the curves for $h/d=1$ are identified by arrows in Fig. 12) we found that a scaling exponent $\eta=2.97$ gives a best fit to the data. Notice that this leaves a very weak dependence on l, the value of which is almost two orders of magnitude smaller than the smallest film thickness considered in this study. What is left is to identify the unknown function of h/d in Eq. (26). For that purpose, we adopt the equality (25) combined with Eq. (26); taking the slopes from Fig. 12(b), we finally find $f(h/d)$ as shown in Fig. 13.

C. No adhesion at the interface

Until now the thin films were considered to be perfectly attached to the substrate. In real systems, bonding is never perfect but depends on the film and substrate materials, processing conditions, likelihood of forming oxide layers, etc. In

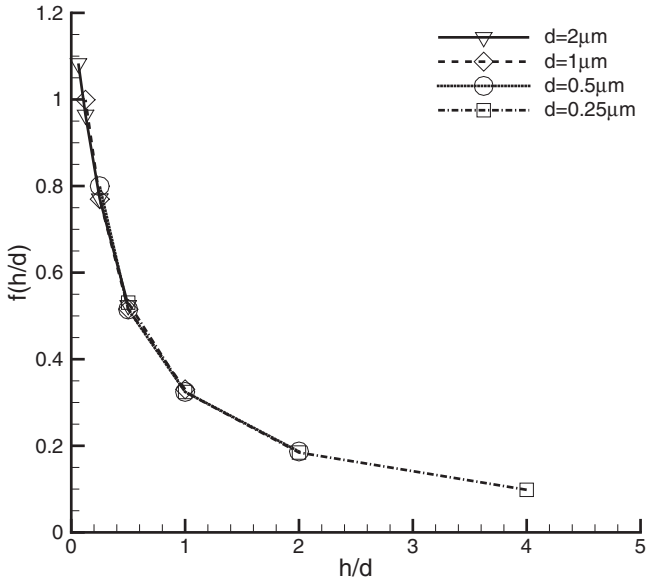

FIG. 13. The function f of grain aspect ratio in the expression (26) for the relaxation time.

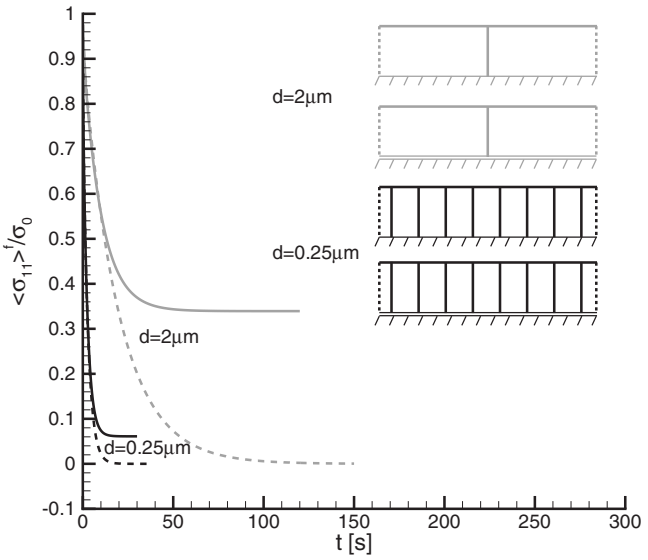

FIG. 15. Relaxation curves for thin films with $h=0.5$ μm. Curves for perfectly bonded interfaces are drawn with solid lines whereas dashed lines are relaxation curves for interfaces with no adhesion.

order to avoid the complexity associated with the interface properties, we will investigate the opposite extreme case, namely where there is no adhesion between film and substrate.

In the absence of adhesion, the boundary conditions of the diffusional and mechanical BVPs change, as depicted in Fig. 14(a). For diffusion, first of all, the constraint on the GB opening $\Delta(0,t)$ disappears since the substrate no longer restricts the sliding of the film over the substrate. The no-flux condition $j_2(0,t)=0$, however, still holds since the GB terminates at $x_2=0$. As for the elasticity of the film, the substrate is no longer relevant. Instead, the tangential tractions along the film's bottom surface should vanish, i.e., $t_1(x_1,0)=0$, while $u_2(x_1,0)=0$ ensures that the film does not lift off.

Before trying to solve this problem, it is noted that these boundary conditions are identical to symmetry conditions for both BVPs about $x_2=0$. Thus, the problem becomes equivalent to that of GB diffusion in a free-standing film with a thickness of $2h$, as illustrated in Fig. 14(b). This interpretation reinforces that the system cannot be loaded with thermal stresses since the thermal expansion of film and substrate can no longer communicate. Therefore we stretch the film in the x_2 direction by superimposing a uniform displacement U_0 at the sides of the cell. The value of U_0 for different grain sizes is chosen such that the corresponding overall initial strain $2U_0/d$ induces the same value of σ_0 in the previous subsections, i.e., $\sigma_0=2E^*U_0/d$.

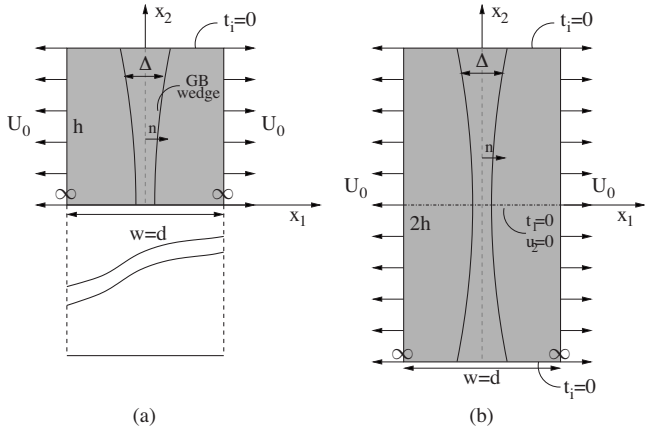

FIG. 14. Schematic of GB diffusion in a periodic cell with thickness h on a substrate in the absence of adhesion (a), and for a free-standing film with thickness $2h$.

The steady state solution of the problem is trivial. Since the constraint on the GB opening at $x_2=0$ is absent, diffusion will continue to eliminate any stress gradient until there is a rectangular GB wedge ($\xi=1$). The final width is equal to the total initial stretch $2U_0$ and the initial applied stress is fully relaxed. In Fig. 15 the relaxation curves for two grain sizes are shown, together with the relaxation curves for perfectly bonded films, for which relaxation is in general not complete. Complete relaxation in the absence of adhesion can be considered as the lower bound for the relaxation, while the perfect-bonding case discussed earlier becomes the upper bound. In reality, since interfaces have a finite strength film delamination may arise due to development of σ_{12} and σ_{22} (see Fig. 9) during diffusion. Thus, the relaxation curves will fall in between these two bounds: close to the lower bound for very weak interfaces where film delamination may be induced during diffusion and close to the upper bound for strong interfaces that do not lead to delamination.

When the kinetics of relaxation in these free-standing films is studied in detail, the same scaling between the characteristic time and film thickness is found as before: $\tau_c \propto h^{2.97}l^{0.03}$. However from Fig. 15 it can be observed that these films reach the steady state slightly later than the perfectly bonded counterparts, meaning that $f(h/d)$ in Eq. (26) is larger than in Fig. 13.

It bears emphasis here that a small change in boundary conditions can give an entirely different problem with different steady state properties and kinetics. For instance, the model of Guduru *et al.*[2] addresses solely the no-flux condi-

tion, so that their solution is for a free-standing film or for a film that is not bonded to the substrate. Incorporating both boundary conditions (10) and (11) for bonded films requires a dedicated treatment of the boundary conditions.

V. CONCLUSIONS

The main conclusions of the two-dimensional modeling of GB diffusion in thin films presented in this work can be summarized as follows.

- GB diffusion is more effective in relaxing the stress in films with slender grains; its effectiveness is characterized by a power law scaling between residual stress and the aspect ratio of grains h/d.
- The effectiveness of relaxation is manifested by the GB wedge shape ξ, and the width of the GB wedge at the top surface, $\Delta(h)$.
- The continuum model predicts relaxation of stress with any magnitude without any threshold and also predicts complete relaxation in the limit of infinite h/d since there is no built-in length scale. Because of this limitation, the continuum model cannot detect the size effects of this phenomena reported in Ref. 3
- The normal stress averaged along the GB decays exponentially with time and becomes zero at the steady state. The characteristic time τ_c scales with film thickness h with an exponent that is very close to 3, and additionally depends on h/d.
- In the absence of adhesion between film and substrate, stress relaxes completely but at a slightly lower pace.

The framework presented here is for stationary films, but can be extended to growing films during deposition. During the growth of metallic films, intrinsic stresses arise as a consequence of competition between diffusion and coalescence of grains. Very recently, Tello and Bower[5] have presented a detailed model in which coalescence stresses are incorporated with a cohesive law along the GB and have investigated this competition in terms of stress development during the Volmer–Weber type growth of polycrystalline films.

ACKNOWLEDGMENTS

This work was supported the European Commission (Sixth Framework) through the STREP project NANOMESO.

[1]H. Gao, L. Zhang, W. D. Nix, C. V. Thompson, and E. Arzt, Acta Mater. **47**, 2865 (1999).
[2]P. Guduru, E. Chason, and L. Freund, J. Mech. Phys. Solids **51**, 2127 (2003).
[3]C. Ayas and E. Van der Giessen, Modell. Simul. Mater. Sci. Eng. **17**, 064007 (2009).
[4]M. J. Buehler, A. Hartmaier, and H. Gao, J. Mech. Phys. Solids **51**, 2105 (2003).
[5]J. S. Tello and A. F. Bower, J. Mech. Phys. Solids **56**, 2727 (2008).